Computerised Tomography of Human Liver Images

Melinda Kovács, Szilvia Nagy
Multidisciplinary PhD School of Engineering Sciences, Széchenyi István University, Egyetem tér 1
Gyor, H-9026 Hungary
Department of Telecommunications at Széchenyi István University, Egyetem tér 1
Gyor, H-9026 Hungary
{nagysz@sze.hu}

ABSTRACT: *Computerised tomography can able to analyse the images of human liver where the statistical parameters are studied using pre-processing methods. This process enables to develop a dataset of intelligent image segmentation and lesion classifying methods with both the liver and the different types of roundish objects within the liver having their own masks as well as their classification. To ensure the validity of the proposed system, the masks can be cross checked, labelled and corrected by medical experts manually, they only give a basis for helping to build the database.*

Keywords: Image Processing, Liver, Computer Tomography, Image Series Database

Received: 26 April 2020, Revised 22 July 2020, Accepted 31 July 2020

DOI: 10.6025/jmpt/2020/11/4/137-144

1. Introduction

Computed tomography was introduced by Godfrey Hounsfield in 1969. It is based on X-ray imaging, a method was used from the beginning of the 20th century, but unlike plain X-ray method, which produces 2D summational images from a body part, computed tomography takes a data map of X-ray absorbing measurements, from which a computer can create 2D or 3D objects. The first use in a real patient was a brain scan in 1971. Hounsfield (and Allan M. Cormack) received the Nobel Prize in Physiology or Medicine in 1979 for the development of computer assisted tomography.

As an essence of the CT machine, an X-ray tube and a detector row are opposed to each other. The detector row is measuring the output beam intensity integrated along a line between X-ray source and detector. It depends from the generation of the given CT machine, whether the X-ray tube is rotating or the detector row, or both, and how many tubes and detector rows are present. Since either the detector or the tube is rotating, data is produced from a given point's X-ray attenuation from many angles, which means that the attenuation of the point can be calculated.

"Tomography" means "imaging by sectioning". From the raw data of thin sections acquired by the machine, a series of algorithms create a thin slice and then a reconstructed image. The mathematical background of CT imaging reconstruction is

the Radon transformation invented in 1917 by Johann Radon, who showed that a function could be reconstructed from an infinite set of its projections [1]. Stefan Kaczmarz developed a method to find an approximate solution to a large system of linear algebraic equations in 1937 [2].

Image reconstruction is a mathematical process that generates visual images from the X-ray attenuation data acquired by the CT machine from many different angles. Image reconstruction has an impact on image quality as well as on the radiation dose. Two major reconstruction method categories are exist. Analytical reconstruction methods are usually based on filtered back projection (FBP), which uses a 1D filter on the projection data before back projecting the data onto the image space. [3]. Iterative Image Reconstruction methods can be found in [4].

Medical imaging uses a special file standard named Digital Imaging and Communications in Medicine (DICOM). It is used for storing and transmitting medical images without data loss. It can be exchanged between to receiving-capable entities. DICOM Conformance Statements state the DICOM classes they support, and the standard includes the definition of the file format, and the protocol for network communication. Every radiological modality has a standard in DICOM [5]. In the case of computer tomography, images are stored usually as matrices of unsigned integers (even though the intensity corresponding to air is –1000 in hounsfield units (HU): everything is shifted by 1000) with dynamic range about 4-5000. The dynamic range of the liver in a CT image is usually not much more than 256. This means, that for image processing purposes, in the case of the liver, standard image formats are also sufficient, and probably more favorable, as the DICOM files have too high dynamic range, they may contain information about the patient and the environment, and they need special readers.

Mostly liver segmentation is done by intelligent systems, that need training sets and tests sets consisting of rather large number of images and masks. Preparation of such a training set is rather time and resource consuming. Also, medical experts are needed for checking and correcting the masks, even if the preparation is done by less qualified staff. Our goal is to provide preliminary masks for both the liver contour and the lesions in order to decrease the human labour need of building databases.

Also, usually independent images are used for image processing purposes, as for larger number of neighbouring images to be studied together much higher computational capacity is necessary. From the point of view of medical experts, however, individual images are usually hardly interpretable, thus it is more favourable to study the series of images in order to be able to determine the nature of the finding.

In this article we are presenting the first steps on building a database. After thresholding the image to the intensity domain of the liver, we apply different kinds of preprocessing methods in order to provide preliminary masks for the liver. As a next step we apply an active contour method for generating a more fitting mask and compare the resulting masks to one another. The applied preprocessing techniques are mean and median filtering, gradient filtering, calculating Rényi entropies for the environment of the pixel and structural entropies.

In Section 2, we summarize the properties of the liver on a CT image of various phases, in Section 3 we give the applied mathematical tools. In Section 4. the results are shown and in Section 5 the results are summarized and a conclusion is drawn.

2. On the CT Images of Human Livers

In diagnosing liver diseases especially tumours, usually contrast material is used, and CT image series are taken before injecting the contrast material (native phase), at the time when the contrast material is mainly in the arteries (arterial phase), at the time, when it is mainly at the veins (portal phase), and later, after ten-fifteen minutes (late phases). The most interesting and informative phases are the arterial and portal ones, though for some differential diagnosis purposes the other phases can be necessary, too.

The liver itself on CT images is a rather diffuse object, with high intensity variation within the organ from pixel to pixel, but generally a rather uniform average intensity throughout the whole organ, except for the blood vessels and the different lesions, like cysts, benign or malignant tumours, as it can be seen in Figure 1.

It seems to be a rather simple thresholding problem to select the liver, however, the dynamic range of the muscle tissue

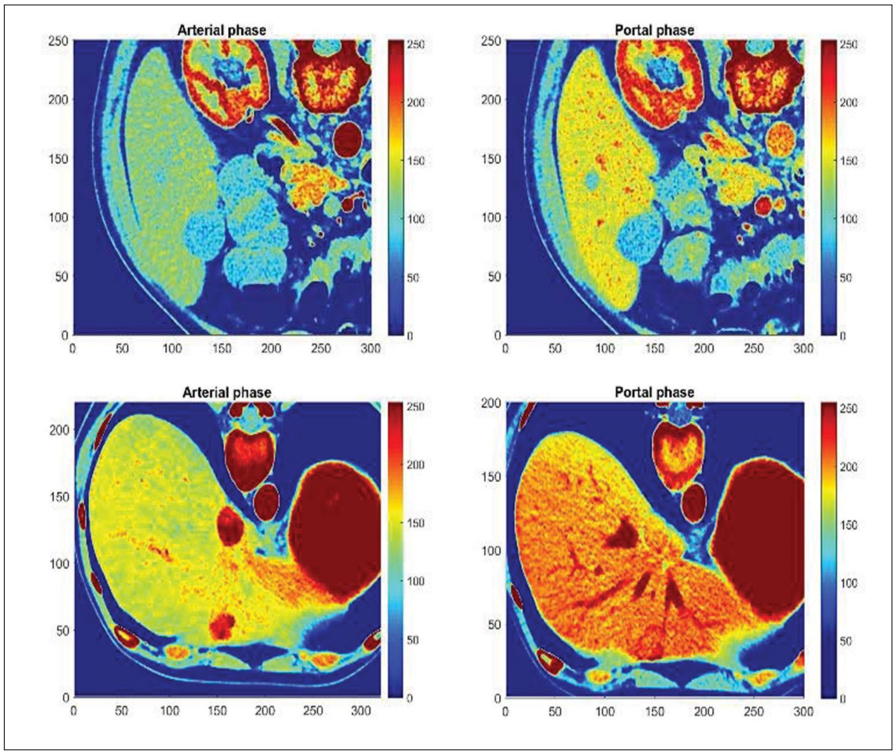

Fig. 1. Arterial and portal phases of two livers with different lesions. The upper row liver has a small cyst around position (90,130), which is more visible at the portal phase. The liver in the lower row has a larger FNH (focal nodular hyperplasia) around position (150, 50), which is more visible at the arterial phase. The scale of the colors is shifted by "50 HU in order to show the most significant 256 HU wide part of the dynamic range, all the units below "50 HU are substituted by 0, and all the levels above 206 HU are substituted by 255

usually overlaps with that of the liver, so it is rather complicated to distinguish between the stomach or blood vessel walls as well as the muscles between the bones and the liver, if they are touching, like in the bottom part of Figure 1.

3. On the Applied Filters

We applied local filters with rather small radius (2, 3 or 5) in order to help the segmentation of the liver from the environment.

3.1 Mean, Median, Standard Deviation, Gradient

As a first step, we studied the mean and median filtered versions of the images. As awaited, they make the liver rather homogeneous, with small variation. We used the difference of the two filtered images, as it can be seen in Figure 2., as the first possible tool for finding the borderlines of the liver and the lesions within.

Also, the standard deviation was used similarly to the mean and median operations in a 5×5 sliding window: this was our second candidate for aiding the segmentation.

Gradients are usually the basis of edge detections, so we also applied gradient filters to the images. Their results can be seen in Fig 2. for the first subplot in Fig. 1. Both the gradient and the deviation are large at the borderlines of the liver and the tumor, while they remain rather small, but significantly larger than zero at the healthy liver parts.

3.2 Entropies

Also, the Rényi entropy based structural entropy and the filling factor was used as in sliding windows of size 5 by 5, similarly to the previous cases.

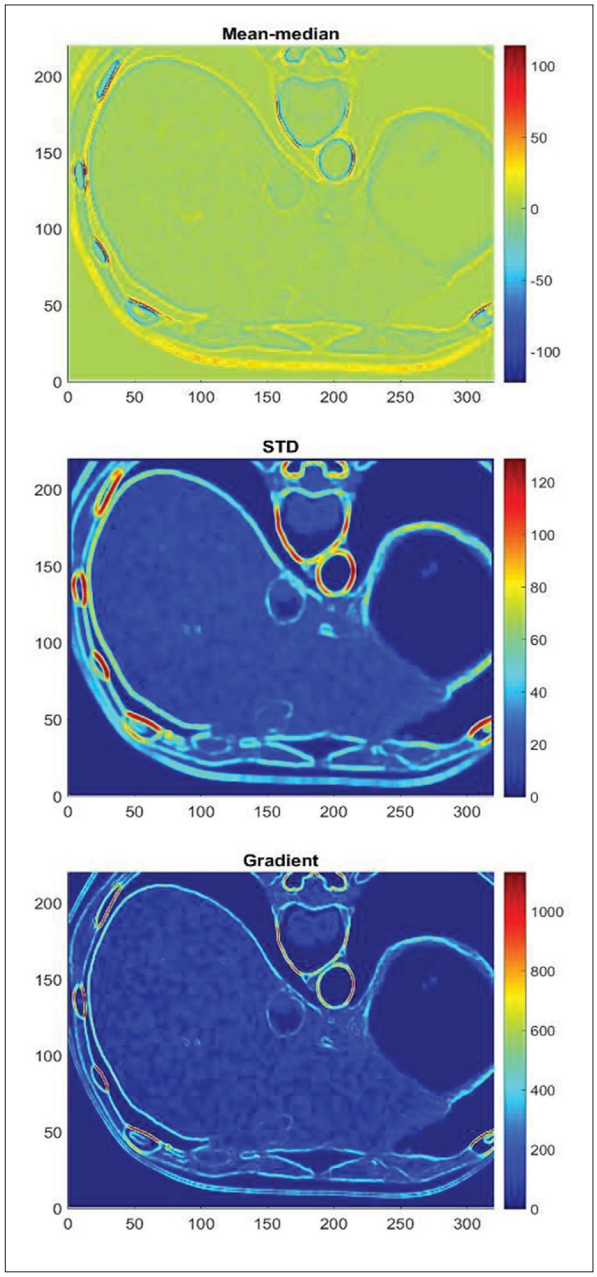

Figure 2. Filtered versions of the third subfigure of Figure 1 with the difference of mean and median filtered image, the standard deviation and gradient filters

The Rényi entropy

$$S_n = \frac{1}{1-n} \ln\left(\sum_{i=1}^{N} I_i{}^n\right) \tag{1}$$

was introduced by Alfréd Rényi [7] and proved to be an extension of Shannon's entropy definition. Pipek and Varga used the differences of Rényi entropies, namely the structural entropy and the logarithm of the spatial filling factor to characterize

$$S_{str} = S_1 - S_2, \tag{2}$$

$$-\ln q = S_0 - S_2, \tag{3}$$

the localization type, i.e., the average shape of electron distributions [8-10]. These quantities were generalized for any type of probability distributions and used for characterizing microscopy [11-13] and surface scanner images [14]. They were also applied antecedents in colonoscopy image analysis [15-17], based on the fuzzy classification method of [18-20]. Generally it can be said that for distributions with rapid decrease the structural entropy is larger, or the logarithm of the filling factor is smaller compared to distributions with less steep slopes.

In Figure 3, as an example, the 1st and 2nd Rényi entropy filtered versions of the third image in Fig. 1 are given together with the structural entropy (2). (The zeroth Rényi entropy is constant, this is why the image from a filter based on (3) is not shown).

3.3 Thresholding and Active Contour

Usually the patients are diagnosed based on the ALARA principles, i.e., the radiation should be "As Low As Reasonably Achievable", which means that for some cases only one phase is available, in some cases more, depending on the purpose of the diagnosing process. As it can be seen from Figure 1, the liver itself is much more separable in the portal phase image. Therefore we suggest starting the segmentation of the liver from the portal phase, if available.

The lesions however might not be distinguishable and very probably they are not diagnosable from a single phase only, this is why we suggest searching for smaller, roundish objects from the arterial and also the later phases as well.

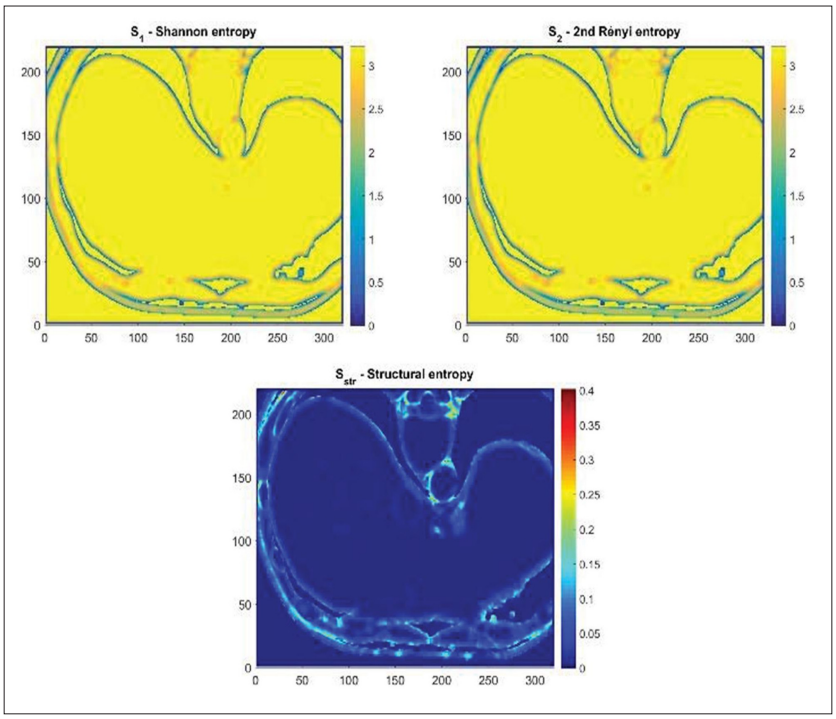

Figure 3. Filtered versions of the third subfigure of Figure 1 with Rényi entropies and structural entropy

The first step for creating masks for the lesions is to provide a mask for a liver in order to limit the search to its area. Using a rather simple thresholding can mark the liver area rather well. If two masks are used, one for giving the area above the muscle tissue level, i.e., a lower mask, and one for filtering out the too high intensities (the bones, blood vessels, stomach or bowel content, etc.), their difference can be used as a basic mask for the liver and the blood vessels, stomach and other objects that are separated from the liver by a non-masked area. These later objects can be eliminated from the mask by an area filling algorithm, while the others usually have thin wall, which can be the basis of the separation, though this tends to leave not nice artifacts.

Using the area filled mask as a basis of an active contour algorithm [21,22] can provide more precise masks.

4. Results

For the basis of the lower and upper masks mentioned in the previous subsection, the median filtered images are of much more use than the original or mean filtered versions, as it can be seen in the example in Figure 4.

The area filling segmentation algorithm needs a point that is within the boundaries of the liver. Although people differ in size, points in the liver can be found, moreover, a basic form corresponding to the liver could also be found, similarly to [21] in order to have a larger starting are for the filling algorithms.

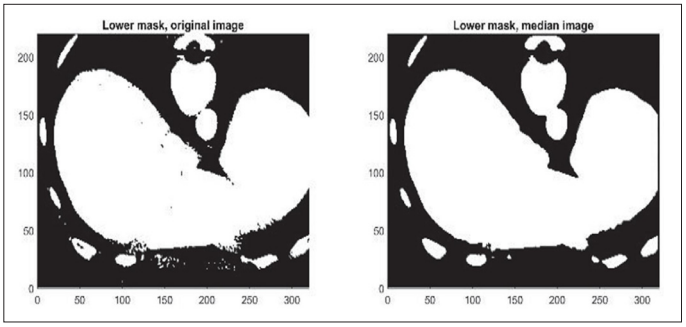

Figure 4. Lower mask from the original and from the median filtered images. The threshold level is at 100 HU

The conditions for quitting the filling for a line can be based on all the filtered images given in the previous section, however, the most effective one seems to be the gradient combined with the median and the structural entropy forming a condition:

• Median larger than a threshold (100 HU), or some of the few neighbors from the center of the area are larger than the threshold.

• Gradient between the limits (10 and 200 HU).

• Structural entropy decreasing to a small number (almost 0, e.g. 0.01) from its first local maximum from the center of the area.

The combination of these three conditions can give rather nice segmentations, as it is visible in the example in Figure 5.

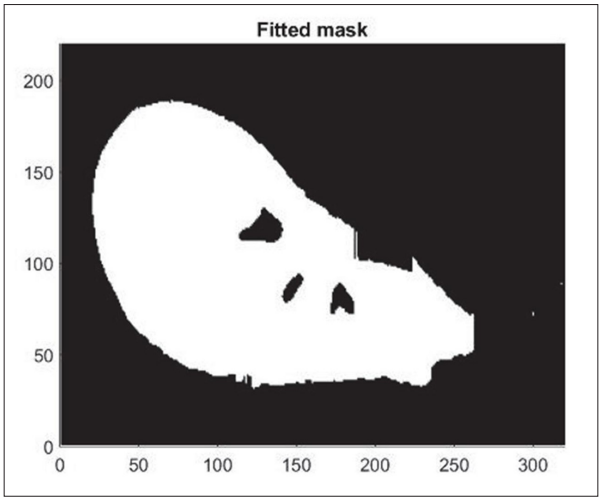

Figure 5. Segmentation mask for the liver after active contour

5. Summary and Conclusion

Basics of a method for providing automatic masks for liver CT images is given. The masks are to be supervised manually in order to provide a database for machine learning algorithms and diagnostics based on computational intelligence methods.

The masks for the liver are generated from a threshold mask based on median filtered portal phase images, using area filling from a starting liver point. The conditions for filling can be based on several processed versions of the image, from gradient and standard deviation filtered to Rényi entropy filtered images. A combination of filling conditions is given using the median filtered image as well as the gradient and structural entropy images for determining the borderlines of the liver.

For segmentation of the lesions within the area of the liver, similar methods can be used: higher and lower median density roundish spots are to be searched.

References

[1] Hornich, H. (1986). Translated by PC. Parks A Tribute to Johann Radon. *IEEE Trans. Med. Imaging*. 5 (4) 169-169. DOI: 10.1109/TMI.1986.4307774.

[2] Kaczmarz, S. (1993). Approximate solution of system of linear equations, *International Journal of Control*, 57 (6) 1269-1271, DOI: 10.1080/00207179308934446.

[3] Kak, A. C., Slaney, M. (1987). *Principles of Computed Tomographic Imaging*. SIAM, Philadelphia, PA.

[4] Hsieh, J. (2009). *Computed Tomography: Principles, Design, Artifacts, and Recent Advances*, 2nd ed: SPIE Press, Bellingham, Washington.

[5] Kahn Jr, C. E., Carrino, J. A., Flynn, M. J., Peck, D. J., Horii, S. C. (2007). DICOM and radiology: past, present, and future. *Journal of the American College of Radiology*. 4 (2) 652-657. DOI 10.1016/j.jacr.2007.06.004

[6] Flanders, A. E., Carrino, J. A. (2003). Understanding DICOM and IHE. *Seminars in Roentgenology*. Vol 38, p. 270–281.

[7] Rényi, A. (1960). On measures of information and entropy. In Proceedings of the fourth Berkeley Symposium on Mathematics, Statistics and Probability, Berkeley, CA, USA, 20 June–30 July, p. 547–561.

[8] Pipek, J., Varga, I. (1992). Universal classification scheme for the spatial localization properties of one-particle states in finite ddimensional systems, *Physical Review A*, Volume 46, APS, Ridge NY-Washington DC, p. 3148—3164.

[9] Varga, I., Pipek, J. (2003). Rényi entropies characterizing the shape and the extension of the phase space representation of quantum wave functions in disordered systems, *Physical Review E*, Vol 68, APS, Ridge NY-Washington DC, 026202.

[10] Nagy, Sz., Sziová, B., Pipek, J. (2019). On Structural Entropy and Spatial Filling Factor Analysis of Colonoscopy Pictures, *Entropy*, Vol 21 (3), ID: 256, 32 pages.

[11] Molnár, L. M., Nagy, Sz., Mojzes, I. (2010). Structural entropy in detecting background patterns of AFM images, Vacuum, Vol 84, Elsevier, Amsterdam, p. 179-183.

[12] Bonyár, A., Molnár, L. M., Harsányi, G. (2012). Localization factor: a new parameter for the quantitative characterization of surface structure with atomic force microscopy (AFM), MICRON, Vol 43, Elsevier, Amsterdam, p. 305-310.

[13] Bonyár, A. (2016). AFM characterization of the shape of surface structures with localization factor. Micron, 87, 1–9.

[14] Solecki, L., Nagy, Sz. (2016). Wavelet Analysis and Structural Entropy Based Intelligent Classification Method for Combustion Engine Cylinder Surfaces, *In*: Proceedings of the 8th European Symposium on Computational Intelligence and Mathematics, ESCIM, 5-8th October, Sofia p. 115-120.

[15] Nagy, Sz., Lilik, F., Kóczy, L. T. (2017). Entropy based fuzzy classification and detection aid for colorectal polyps. *In*: Proceedings of the IEEE Africon, Cape Town, South Africa, 18– 20 September, p. 78–82.

[16] Nagy, Sz., Sziová, B., Kóczy, L. T. (2018). The effect of image feature qualifiers on fuzzy colorectal polyp detection schemes using KH interpolation - towards hierarchical fuzzy classification of coloscopic still images. *In*: Proceedings of the FuzzIEEE, Rio de Janeiro, Brazil, 8–13 July, p. 1–7.

[17] Nagy, Sz., Sziová, B., Solecki, L. (2019). The effect of background and outlier subtraction on the structural entropy of

two-dimensional measured data, under publication at IJRIS.

[18] Lilik, F., Botzheim, J. (2011). Fuzzy based Prequalification Methods for EoSHDSL Technology. *Acta. Tech. Jaurinensis*, Vol 4, p. 135–144.

[19] Lilik, F., Kóczy, L. T. (2013). Performance Evaluation ofWire Pairs in Telecommunications Networks by Fuzzy and Evolutionary Models. *In*: Proceedings of the IEEE Africon, Pointe-Aux- Piments, Mauritius, 9–12 September, p. 712–716.

[20] Lilik, F., Nagy, Sz., Kóczy, L.T. (2018). Improved Method for Predicting the Performance of the Physical Links in Telecommunications Access Networks. *Complexity*, Article ID 3685927.

[21] Mihaylova, A., Georgieva, V. (2018). Spleen segmentation in MRI sequence images using template matching and active contours *Procedia Computer Science*. Vol 131, p. 15-22.

[22] Georgieva, V., Ermakov, S. (2016). GUI for CT image segmentation via active contours, 2016 IEEE International Black Sea Conference on Communications and Networking (BlackSeaCom).